Single-phase-to-ground Fault Detection with Distributed Parameters Analysis in Non-direct Grounded Systems

Baowen Liu, *Student Member, IEEE,* Hongzhong Ma, *Member, CSEE*, Honghua Xu, and Ping Ju, *Senior Member, IEEE*

***Abstract*—The fast and accurate detection of the single-phase-to-ground fault is of great significance for the reliability and safety of the power supply. In this paper, novel algorithms for distribution network protection were proposed with distributed parameters analysis in non-direct grounded systems. At first, novel generating mechanisms of zero-sequence voltage and residual current were proposed. Then the compositions of residue parameters, including residual current and residual admittances, were decomposed in detail. After that, an improved algorithm for a fault resistance calculation of a single phase-to-earth fault was also proposed, and the algorithm is much more convenient as it only needs to measure the variation of the zero-sequence voltage and dows not need the prerequisites of the faulty feeder selection. Still further, the fault feeder can also be selected by an improved calculation algorithm of zero-sequence admittance of the faulty feeder, which cannot be affected by the asymmetry of the network. Theoretical analysis and the MATALB/Simulink simulation results demonstrate the effectiveness of the proposed algorithms.**

***Index Terms*—**Non-direct grounded system, fault resistance calculation, fault feeder selection, residual parameters, residual current, zero-sequence voltage

I. Introduction

Most prone to fault in power systems are the distribution lines, and a large majority of which are generally single-phase-to-ground faults. Power distribution lines have represented an extremely important role in achieving the necessary continuity of service from substations to customers [1]. As the fault current is small and the line-to-line voltage remains constant, the supply of electric power can be maintained for a long time when the single-phase-to-ground fault occurs in high impedance grounded networks which have been widely used in Europe and Asia [2], [3].

In compensation grounding systems, as the Petersen coil produces inductive current at the neutral point of the network to compensate the capacitive fault current, the detection of a single-phase-to-ground fault is more difficult than that in solid grounded systems. And then, the zero-sequence over the current protection algorithm and zero-sequence captive current direction based protection algorithm are no longer applicable in compensated networks [4]–[6]. But the grounding fault protection algorithm based on the active component direction of the zero sequence current cannot be influenced by the compensation of the Petersen coil [7]. However, compared with the residual current in the feeder, the active component is small, let alone the low-current faults are produced by high fault resistance. So the sensitivity of the conventional detection algorithm was low [7]. In addition, the active component of the zero-sequence current can also be influenced a lot by the asymmetry of the networks, especially in high resistance ground faults.

The most important steady state data based algorithms for single-phase-to-ground fault detection are DESIR (Detection Sélective par des Intensités Residuéls/“Selective Detection using Residual Currents”) and DDA (Differential Detection using phase-to-ground Admittances) [2], [6]–[8]. These algorithms are generally based on calculating and monitoring the resistances of each phase and feeder, partial residual neutral voltages, relative variations of the line asymmetries and phase asymmetries [9], [10]. In addition, there is an algorithm based on the change of the neutral-voltage and zero-sequence currents [11]. However, these algorithms present a limitation with their application in the certain grounding systems [1]. Reference [1] proposes a new method of detecting the low-current faults based on monitoring the residual variations of the line and phase asymmetries, which can be used in both compensated and ungrounded mid-voltage networks. As the magnitude of line and phase asymmetry is small, it is difficult to obtain accurate measurement results.

There are also several methodologies proposed to detect single-phase earth faults, including artificial-intelligence (AI) techniques [12], [13], Laplace trend statistics (LTS) [14], and transient-state data analysis (TDA) (e.g., wavelet transform, traveling wave, etc.) [15]–[18]. All these methodologies have improved the detection of single-phase-to-ground fault, but each has its own shortcomings, such as, AI and LTS based techniques are still not yet mature enough for implementation in various conditions, and TDA based techniques needs more complicated algorithms to practically discriminate between before and during faults [5], [15].

In this paper, novel generating mechanisms of zero-sequence voltage and residual current are first proposed. According to the novel generating mechanisms, the compositions of the residual current and residual admittance can be decomposed in detail, and the influence of the feeder’s asymmetry is considered. Then the single-phase-to-ground fault protection algorithms are proposed, which include the fault resistance measurement and fault feeder selection. And the effectiveness of the proposed component analysis of residual parameters and earth fault protection algorithms are

Manuscript received July 24, 2016; revised January 10, 2017; accepted April 10, 2017. This work was supported in part by the National Natural Science Foundation of China (51177039), in part by Innovative Research Project for Postgraduates in Colleges of Jiangsu Province(KYLX15_0481), Fundamental Research Funds for the Central Universities (2015B37014), and in part by the Science and Technology Project of Jiangsu Electric Power Corporation (J2014055, J2015054).

B. W. Liu (corresponding author, e-mail: lbw_5566@163.com), H. Z. Ma, and P. Ju are with the College of Energy and Electrical Engineering, Hohai University, Nanjing 211100, China.

H. H. Xu is with the State Grid Jiangsu Electric Power Company Nanjing Power Supply Company, Nanjing 210008, China.

DOI: 10.17775/CSEEJPES.2016.00740

validated by the MATALB/Simulink simulations.

II. Novel Generating Mechanisms of Zero-sequence Voltage and Residual Current

A. Zero-sequence Voltage Generating Mechanism

Strictly speaking, the distribution parameters of feeders in non-direct grounded networks are asymmetrical, which is decided by the feeders' laying form and structure. If all feeders of a network are cable, the range of the asymmetry coefficient is 0.2%–0.5%; if all feeders are overhead lines with transposition, the range of the asymmetry coefficient is 0.5%–1.5%; and if the overhead lines are without transposition, the range of the asymmetry coefficient is 1.5%–5% [19], [20].

Consider the simplified equivalent circuit of non-direct grounded systems with 1 feeder shown in Fig. 1, where C_A, C_B, C_C are the phase-to-earth capacitance, respectively; G_A, G_B, G_C are the phase-to-earth conductance, respectively; $\dot{Y}_0$ is the neutral grounding admittance.

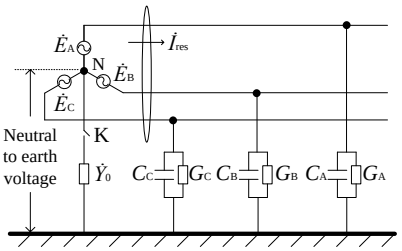

Fig. 1. Insulation parameters measuring circuit

1) In Solid Grounded Systems

In solid grounded systems, the neutral-to-earth voltage is 0. The residual current $\dot{I}_{res}$ can be calculated as:

$$\begin{aligned}\dot{I}_{res} &= \dot{I}_{bd} = \dot{E}_A\dot{Y}_A + \dot{E}_B\dot{Y}_B + \dot{E}_C\dot{Y}_C \\ &= \dot{E}_A(\dot{Y}_A + \alpha^2\dot{Y}_B + \alpha\dot{Y}_C) \\ &= \dot{E}_A\dot{k}_0\end{aligned} \tag{1}$$

where $\dot{Y}_A = j\omega C_A + G_A$, $\dot{Y}_B = j\omega C_B + G_B$, $\dot{Y}_C = j\omega C_C + G_C$; α^2 and α are the rotation operators ($2\pi/3$, $4\pi/3$, respectively) in the complex plane; $\dot{k}_0$ is the natural unbalanced parameters of the feeder; $\dot{I}_{bd}$ is the natural unbalance current. $\dot{I}_{bd}$ and $\dot{k}_0$ are only determined by the structure of the network. If the distribution parameters of the whole network are symmetrical, $\dot{I}_{bd} = 0$.

2) In Ungrounded Systems

For the ungrounded systems, the switch K shown in Fig.1 is off. As is widely known, there is no residual current in ungrounded systems. But the natural unbalance current is not 0 (i.e., $\dot{I}_{bd} \neq 0$). In order to meet Kirchhoff's current law, the network should generate the zero-sequence voltage at the neutral point adaptively. As the neutral-to-earth voltage in ungrounded systems is only determined by the asymmetry of the line distributed parameters, the neutral-to-earth voltage $\dot{U}_{bd}$ in ungrounded systems can also be named as the natural unbalanced voltage.

The current $\dot{I}_{Ubd}$ produced by the natural unbalanced voltage $\dot{U}_{bd}$ on the total zero-sequence impedance is:

$$\dot{I}_{Ubd} = \dot{U}_{bd}\dot{Y}_{\Sigma 0} \tag{2}$$

where $\dot{Y}_{\Sigma 0}$ is the total zero-sequence admittance of the ungrounded system, $\dot{Y}_{\Sigma 0} = j\omega C_\Sigma + G_\Sigma$, $C_\Sigma = C_A + C_B + C_C$, and $G_\Sigma = G_A + G_B + G_C$. According to Kirchhoff's current law, $\dot{I}_{Ubd}$ should satisfy the equation:

$$\dot{I}_{Ubd} + \dot{I}_{bd} = 0 \tag{3}$$

From (1)–(3), in ungrounded systems, the natural unbalanced voltage $\dot{U}_{bd}$ can be calculated as:

$$\dot{U}_{bd} = -\frac{\dot{I}_{bd}}{\dot{Y}_{\Sigma 0}} = -\frac{\dot{E}_A\dot{k}_0}{j\omega C_\Sigma + G_\Sigma} \tag{4}$$

Equation (4) is the same as the formula in [21] calculated by using Kirchhoff's voltage law.

3) In Non-direct Grounded Systems

The non-direct grounded systems include ungrounded, impedance grounded, and resonant grounded systems. The total zero sequence admittance of the non-direct grounded network is $\dot{Y}_{Y\Sigma} = j\omega C_\Sigma + G_\Sigma + \dot{Y}_0$. Due to the introduction of the grounding admittance, if $\dot{Y}_0 \neq 0$, it is obvious that the neutral-to-earth voltage $\dot{U}_0$ in non-direct grounded systems is different from the natural unbalanced voltage $\dot{U}_{bd}$ in ungrounded systems. The current produced by the neutral-to-earth voltage $\dot{U}_0$ on the total zero-sequence impedance is $\dot{I}_{U0} = \dot{U}_0\dot{Y}_{Y\Sigma}$. However, the natural unbalance current $\dot{I}_{bd}$ has nothing to do with the neutral grounding admittance $\dot{Y}_0$. According to Kirchhoff's current law, $\dot{I}_{U0}$ should satisfy the equation as:

$$\dot{I}_{U0} + \dot{I}_{bd} = 0 \tag{5}$$

From (1) and (5), in non-direct grounded networks, the neutral-to-earth voltage $\dot{U}_0$ can be calculated as:

$$\dot{U}_0 = -\frac{\dot{I}_{bd}}{\dot{Y}_{Y\Sigma}} = -\frac{\dot{E}_A\dot{k}_0}{j\omega C_\Sigma + G_\Sigma + \dot{Y}_0} \tag{6}$$

Through the above derivation we can form a novel generating mechanism of neutral-to-earth voltage in the power network and its physical meaning are expounded: asymmetrical power network produces the neutral-to-earth voltage adaptively, and the current produced by the neutral-to-earth voltage on the total zero-sequence impedance compensates the natural unbalance current completely. So, the neutral-to-earth voltage is controlled by the total zero-sequence impedance and the natural unbalance current, jointly.

B. Residual-current Generating Mechanism

In practice, the residual current exists in asymmetrical networks. The generation condition of the residual current is that the zero-sequence voltage is not equal to the natural unbalanced voltage of the feeder. For the ungrounded network with several feeders, the residual current exists in each feeder, but the sum of the residual currents of all feeders is 0.

From (1)–(3), the residual current of the solid grounded feeder can be rewritten as:

$$\begin{aligned}\dot{I}_{res} &= \dot{I}_{bd} = (\dot{U}_0 - \dot{U}_{bd})(j\omega C_\Sigma + G_\Sigma) \\ &= \dot{U}_{\Delta res}(j\omega C_\Sigma + G_\Sigma)\end{aligned} \tag{7}$$

where $\dot{U}_{\Delta res}$ is named as the residual voltage, which indicates the deviation of the zero-sequence voltage $\dot{U}_0$ from the natural unbalanced voltage $\dot{U}_{bd}$.

Analogously, the residual current $\dot{I}_{res}$ of the non-direct grounded system is equal to the neutral-to-earth current, as:

$$\dot{I}_{res} + \dot{I}_{Y0} = 0 \tag{8}$$

From (4), (6) and (8), $\dot{I}_{res}$ can be calculated as:

$$\begin{aligned} \dot{I}_{res} &= -\dot{I}_{Y0} = (\dot{U}_0 - \dot{U}_{bd})(j\omega C_\Sigma + G_\Sigma) \\ &= \dot{U}_{\Delta res}(j\omega C_\Sigma + G_\Sigma) \end{aligned} \tag{9}$$

As can be seen from (7) and (9), despite the grounding modes being different, the calculation form of the residual currents are the same. Through the above derivation we can form a novel generating mechanism of the residual current in the power network and its physical meaning are expounded: asymmetrical power network produces the residual current adaptively, and the current produced by the residual voltage $\dot{U}_{\Delta res}$ on the zero-sequence impedance of the feeder is residual current. So, the residual current is controlled by the zero-sequence impedance and the residual voltage, jointly.

Residual voltage can be changed by injecting the fundamental frequency current at the neutral-to-earth point [1] ,[7], [22], or by adjusting the neutral-to-earth impedance, such as the Petersen coil [23], [24].

III. Component Analysis of Residual Parameters

A. Component Analysis of Residual Current

According to the static version of DESIR [1], [6], [7], [25], in the earth fault state, the residual current of the feeders was considered as the sum of two independent parts. One part is the sum of the phase-to-ground capacitive, and other part is dependent on the asymmetry of the distribution parameters. However, the leakage resistances of the feeders in the static version of DESIR were neglected. Actually, the damping coefficient *d* usually changes from 3% to 5%, which depends on the feeder's age, environmental humidity, temperature, etc [1], [2], [19], [20].

A more detailed component analysis of the residual current is presented below.

1) In the Normal State

Consider the simplified equivalent circuit of a radial operated distribution system with *n* feeders shown in Fig.2. According to the generating mechanisms of the zero-sequence voltage and residual current proposed above, zero-sequence voltage $\dot{U}_0$ of a distribution system with *n* feeders in the normal state can be calculated as:

$$\dot{U}_0 = -\frac{\dot{I}_{bd\Sigma}}{\dot{Y}_{Y\Sigma}} = -\frac{\dot{E}_A \dot{k}_\Sigma}{j\omega C_\Sigma + G_\Sigma + \dot{Y}_0} \tag{10}$$

where $\dot{I}_{bd\Sigma}$ is the sum of the natural unbalance current of each feeder, $\dot{I}_{bd\Sigma} = \sum_{i=1}^{n} \dot{I}_{bdi}$ (i=1,2,⋯,n), $\dot{I}_{bdi}$ is the natural unbalance current of the feeder *i*, $\dot{k}_\Sigma$ is the sum of the natural unbalanced parameters of all feeders, $\dot{k}_\Sigma = \sum_{i=1}^{n} \dot{k}_i$, $\dot{k}_i$ is the natural unbalanced parameters of the feeder (i=1,2,…,n). The natural unbalanced voltage of the feeder *i* can be written as:

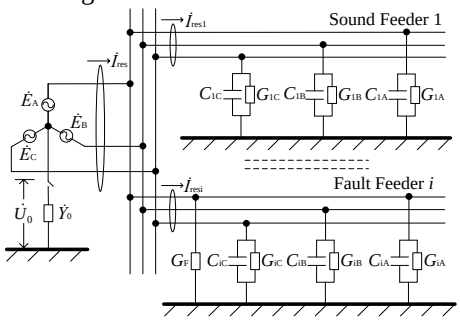

Fig. 2. Simplified equivalent circuit of a radial operated distribution system with a faulty feeder

$$\dot{U}_{bdi} = -\frac{\dot{I}_{bdi}}{\dot{Y}_{\Sigma i}} = -\frac{\dot{E}_A \dot{k}_i}{j\omega C_{\Sigma i} + G_{\Sigma i}} \tag{11}$$

where $\dot{Y}_{\Sigma i}$ is the zero-sequence admittance of the feeder *i*, $C_{\Sigma i}$ is the total distributed capacitance of the feeder *i*, and $G_{\Sigma i}$ is the total distributed conductance of the feeder *i*. The residual current $\dot{I}_{resi}$ of the feeder *i* and the total residual current $\dot{I}_{res\Sigma}$ of the system can be written respectively, as:

$$\dot{I}_{resi} = (\dot{U}_0 - \dot{U}_{bdi})(j\omega C_{\Sigma i} + G_{\Sigma i}) \tag{12}$$

$$\dot{I}_{res\Sigma} = (\dot{U}_0 - \dot{U}_{bd})(j\omega C_\Sigma + G_\Sigma) \tag{13}$$

As the asymmetry of each feeder is random and independent, each feeder always has residual current.

From (10)–(12), the residual current of the feeder *i* in (12) can be rewritten as:

$$\dot{I}_{resi} = -\dot{\tau}_i \dot{I}_{bd\Sigma} + \dot{I}_{bdi} \tag{14}$$

where $\dot{\tau}_i$ is the quotient, and $\dot{\tau}_i = \dot{Y}_{\Sigma i} / \dot{Y}_{Y\Sigma}$. From (14), in the normal state of the network, the residual current of a feeder is the sum of two independent parts. One part is the natural unbalance current $\dot{I}_{bdi}$ of the feeder, and the other part is proportional to the total natural unbalance current $\dot{I}_{bd\Sigma}$ of the network. Through the above derivation, in the normal state of the network, the small-random residual current of a feeder is determined not only by the natural unbalance of itself, but also by the natural unbalance of the whole system.

The sum residual current of all feeders in (13) can be rewritten as:

$$\dot{I}_{res\Sigma} = \sum_{i=1}^{n} \dot{I}_{resi} = \dot{\tau}_\Sigma \dot{I}_{bd\Sigma} \tag{15}$$

where $\dot{\tau}_\Sigma = \dot{Y}_0 / \dot{Y}_{Y\Sigma}$, and $\dot{I}_{res\Sigma} = -\dot{U}_0 \dot{Y}_0$.

2) In the Single-phase-to-ground Fault State

If the single-phase-to-ground fault is represented by a transition conductance G_F in feeder *i*, the zero-sequence voltage $\dot{U}_{0F}$ can be calculated as:

$$\dot{U}_{0F} = -\frac{\dot{I}_{bd\Sigma} + \dot{I}_{bdF}}{\dot{Y}_{Y\Sigma} + G_F} = -\frac{\dot{E}_A \dot{k}_\Sigma + \dot{E}_A G_F}{j\omega C_\Sigma + G_\Sigma + \dot{Y}_0 + G_F} \tag{16}$$

where $\dot{I}_{bdF}$ is the unbalance current caused by the transition conductance G_F, $\dot{I}_{bdF} = \dot{E}_A G_F$. And the natural unbalanced voltage of the fault feeder *i* is:

$$\dot{U}_{\mathrm{bdF}i}=-\frac{\dot{I}_{\mathrm{bd}i}+\dot{I}_{\mathrm{bdF}}}{\dot{Y}_{\Sigma i}+G_{\mathrm{F}}}=-\frac{\dot{E}_{\mathrm{A}}\dot{k}_i+\dot{E}_{\mathrm{A}}G_{\mathrm{F}}}{\mathrm{j}\omega C_{\Sigma i}+G_{\Sigma i}+G_{\mathrm{F}}} \tag{17}$$

The residual current of the fault feeder *i* and the sound feeder 1 can be written respectively, as:

$$\dot{I}_{\mathrm{res}Fi}=(\dot{U}_{0\mathrm{F}}-\dot{U}_{\mathrm{bdF}i})(\mathrm{j}\omega C_{\Sigma i}+G_{\Sigma i}+G_{\mathrm{F}}) \tag{18}$$

$$\dot{I}_{\mathrm{res}S1}=(\dot{U}_{0\mathrm{F}}-\dot{U}_{\mathrm{bd}1})(\mathrm{j}\omega C_{\Sigma 1}+G_{\Sigma 1}) \tag{19}$$

From (16)–(18), the residual current of the fault feeder *i* in (18) can be rewritten as:

$$\dot{I}_{\mathrm{res}Fi}=-\dot{\tau}_{\mathrm{F}i}\dot{I}_{\mathrm{bd}\Sigma}+(1-\dot{\tau}_{\mathrm{F}i})\dot{I}_{\mathrm{bdF}}+\dot{I}_{\mathrm{bd}i} \tag{20}$$

where $\dot{\tau}_{\mathrm{F}i}=(\dot{Y}_{\Sigma i}+G_{\mathrm{F}})/(\dot{Y}_{\mathrm{Y}\Sigma}+G_{\mathrm{F}})$. Likewise, the residual current of the sound feeder 1 in (19) can be rewritten as:

$$\dot{I}_{\mathrm{res}S1}=-\dot{\tau}_{\mathrm{S}1}\dot{I}_{\mathrm{bd}\Sigma}-\dot{\tau}_{\mathrm{S}1}\dot{I}_{\mathrm{bdF}}+\dot{I}_{\mathrm{bd}1} \tag{21}$$

where $\dot{\tau}_{\mathrm{S}1}=\dot{Y}_{\Sigma i}/(\dot{Y}_{\mathrm{Y}\Sigma}+G_{\mathrm{F}})$. From (20) and (21), the residual current in the fault network is the sum of three independent parts. One part is the natural unbalance current of the feeder, the second part is proportional to the total natural unbalance current of the system $\dot{I}_{\mathrm{bd}\Sigma}$, and the third part is proportional to the unbalance current caused by the transition conductance $\dot{I}_{\mathrm{bdF}}$.

If the single-phase-to-ground fault is metallic, $G_{\mathrm{F}}\to\infty$, the unbalance introduced by the earth fault is considerably greater than the natural unbalances of the feeder. (20) and (21) which can be rewritten as:

$$\dot{I}_{\mathrm{res}Fi}=-\dot{I}_{\mathrm{bd}\Sigma}+\dot{I}_{\mathrm{bd}i} \tag{22}$$

$$\dot{I}_{\mathrm{res}S1}=\dot{I}_{\mathrm{bd}1} \tag{23}$$

From (22) and (23), in the metallic single-phase-to-ground fault, the residual current of the sound feeder is equal to its natural unbalance current, and the residual current of the faulty feeder is equal to the negative sum of all sound feeders' natural unbalance current. Then, the fault feeder can be selected. But, with low accuracy introduced by the asymmetry of the network, this method cannot be used in the condition of the high- resistance-ground fault.

B. Component Analysis of Residual Admittance

In the static version of DESIR [1], [6], [7], [25], the residual current of the healthy feeders were considered as perpendicular to the zero-sequence voltage. By analyzing the residual admittance, a fresh judgement of the phase relationship between the residual current and zero-sequence voltage is essential.

1) In the Normal State

The residual admittance of the feeder in this paper is defined as the quotient of the residual current divided by the zero-sequence voltage. In the normal state of the network, the residual admittances $\dot{Y}_{\mathrm{res}S}$ of the sound feeder can be calculated by using (10)–(12), as:

$$\dot{Y}_{\mathrm{res}S}=\frac{\dot{I}_{\mathrm{res}S}}{\dot{U}_0}=\dot{Y}_{\Sigma S}-\frac{\dot{I}_{\mathrm{bd}S}}{\dot{I}_{\mathrm{bd}\Sigma}}\dot{Y}_{\mathrm{Y}\Sigma} \tag{24}$$

From (24), the residual admittance of the sound feeder is the sum of two independent parts. One part is the sum of the zero-sequence admittances of the feeder (i.e., $\dot{Y}_{\Sigma S}$), the other part is proportional to the zero-sequence admittance of the total system (i.e., $\dot{Y}_{\mathrm{Y}\Sigma}$). Furthermore, as the value of $\dot{I}_{\mathrm{bd}S}$ and $\dot{I}_{\mathrm{bd}\Sigma}$ are stochastic, the residual admittance of the feeder can be greatly influenced by the asymmetry of the network.

2) In the Single-phase-to-ground Fault State

If a single-phase-to-ground fault is represented on phase A in feeder *i* by a transition conductance G_{F}, the residual admittance $\dot{Y}_{\mathrm{res}Fi}$ of the fault feeder *i* can be calculated by using (16)–(18), as:

$$\dot{Y}_{\mathrm{res}Fi}=\frac{\dot{I}_{\mathrm{res}Fi}}{\dot{U}_{0\mathrm{F}}}=\dot{Y}_{\Sigma i}-\frac{\dot{I}_{\mathrm{bd}i}+\dot{I}_{\mathrm{bdF}}}{\dot{I}_{\mathrm{bd}\Sigma}+\dot{I}_{\mathrm{bdF}}}\dot{Y}_{\mathrm{Y}\Sigma}+\frac{\dot{I}_{\mathrm{bd}\Sigma}-\dot{I}_{\mathrm{bd}i}}{\dot{I}_{\mathrm{bd}\Sigma}+\dot{I}_{\mathrm{bdF}}}G_{\mathrm{F}} \tag{25}$$

From (25), the residual admittance of the fault feeder is the sum of three independent parts. Likewise, the residual admittances $\dot{Y}_{\mathrm{res}S1}$ of the sound feeder 1 can be calculated as:

$$\dot{Y}_{\mathrm{res}S1}=\frac{\dot{I}_{\mathrm{res}S1}}{\dot{U}_{0\mathrm{F}}}=\dot{Y}_{\Sigma 1}-\frac{\dot{I}_{\mathrm{bd}1}}{\dot{I}_{\mathrm{bd}\Sigma}+\dot{I}_{\mathrm{bdF}}}\dot{Y}_{\mathrm{Y}\Sigma}-\frac{\dot{I}_{\mathrm{bd}1}}{\dot{I}_{\mathrm{bd}\Sigma}+\dot{I}_{\mathrm{bdF}}}G_{\mathrm{F}} \tag{26}$$

From (26), the residual admittance of the sound feeder is also the sum of three independent parts. And the residual admittance of the sound feeder can also be affected by the transition conductance G_{F}. According to the component analysis of the residual admittance, the phase relationship between the residual current and the zero-sequence voltage is complex.

If the single-phase-to-ground fault is metallic, $G_{\mathrm{F}}\to\infty$, the unbalance introduced by the earth fault is considerably greater than the natural unbalance of the feeder. (25) and (26) can be rewritten as:

$$\dot{Y}_{\mathrm{res}Fi}=\frac{\dot{I}_{\mathrm{res}Fi}}{\dot{U}_{0\mathrm{F}}}=\dot{Y}_{\Sigma i}+\dot{k}_i-(\dot{Y}_{\mathrm{Y}\Sigma}+\dot{k}_{\Sigma})\approx\dot{Y}_{\Sigma i}-\dot{Y}_{\mathrm{Y}\Sigma} \tag{27}$$

$$\dot{Y}_{\mathrm{res}S1}=\frac{\dot{I}_{\mathrm{res}S1}}{\dot{U}_{0\mathrm{F}}}=\dot{Y}_{\Sigma 1}-\dot{k}_1\approx\dot{Y}_{\Sigma 1} \tag{28}$$

From (27) and (28), as the unbalanced parameters (i.e., $\dot{k}_i$ and $\dot{k}_{\Sigma}$) are much smaller than the zero-sequence admittance (i.e., $\dot{Y}_{\Sigma i}$ and $\dot{Y}_{\mathrm{Y}\Sigma}$), the residual admittance of the sound feeder is equal to its zero-sequence admittances, and the faulty feeder's residual admittance is equal to the neutral grounding admittance plus the negative sum of all the sound feeders' zero-sequence admittances. In the metallic single-phase-to-ground fault, the residual current of the healthy feeders is almost perpendicular to the zero-sequence voltage. Then, the faulty feeder can be selected. But with low accuracy introduced by the asymmetry of the network, this method also cannot be used in the condition of the high-resistance-earth fault.

IV. Algorithms for Earth Faults Protection

A. Protection Algorithm of Fault Resistance Measurements

The algorithm of DDA can calculate the faulted current and the fault resistance [6] ,[7], [25]. But this algorithm needs some preconditions, such as the fault feeder should be selected correctly and the fault feeder's zero-sequence admittances should be measured accurately. What's more, this algorithm not only needs to measure the variations of the zero-sequence voltage, but also needs to measure the variation of the residual current. Thus, it is complicated. And the DDA algorithm has ignored the leakage conductance in its theoretical model.

From (10)–(12), in the normal state of the network, the natural unbalanced current of the feeder *i* can be rewritten as:

$$\dot{I}_{\mathrm{bd}i} = \dot{I}_{\mathrm{res}i} - \dot{U}_0 \dot{Y}_{\Sigma i} \tag{29}$$

From (16)–(18), if a single-phase-to-ground fault is represented by a transition conductance G_F in feeder *i*, the residual current of the fault feeder *i* can be rewritten as:

$$\dot{I}_{\mathrm{resF}i} = \dot{U}_{0\mathrm{F}} \dot{Y}_{\Sigma i} + \dot{I}_\mathrm{F} + \dot{I}_{\mathrm{bd}i} \tag{30}$$

Where $\dot{I}_\mathrm{F} = (\dot{U}_{0\mathrm{F}} + \dot{E}_\mathrm{A})G_\mathrm{F}$, $\dot{I}_\mathrm{F}$ is the faulted current. From (29) and (30), the faulted current $\dot{I}_\mathrm{F}$ can be calculated as:

$$\begin{aligned} \dot{I}_\mathrm{F} &= \dot{I}_{\mathrm{resF}i} - \dot{I}_{\mathrm{res}i} - (\dot{U}_{0\mathrm{F}} - \dot{U}_0)\dot{Y}_{\Sigma i} \\ &= \dot{I}_{\Delta\mathrm{resF}i} - \dot{U}_{\Delta 0\mathrm{F}} \dot{Y}_{\Sigma i} \end{aligned} \tag{31}$$

where $\dot{I}_{\Delta\mathrm{resF}i}$ is the variation of the residual current caused by the single-phase-to-ground fault; $\dot{U}_{\Delta 0\mathrm{F}}$ is the zero-sequence voltage variation caused by the single-phase-to-ground fault. If the single-phase-to-ground fault occurred on phase A, the fault resistance can be calculated as:

$$R_\mathrm{F} = \frac{\dot{U}_{0\mathrm{F}} + \dot{E}_\mathrm{A}}{\dot{I}_{\Delta\mathrm{resF}i} - \dot{U}_{\Delta 0\mathrm{F}} \dot{Y}_{\Sigma i}} \tag{32}$$

Equation (32) is derived based on the relationship of the residual current and zero-sequence voltage, which is the same as with algorithm DDA [6], [7], [25]. As the theoretical model takes the leakage conductance of the feeder into account, (32) has the advantage of higher accuracy than the DDA algorithm. As the DDA algorithm needs to measure the residual current variation $\dot{I}_{\Delta\mathrm{resF}i}$ of the fault feeder, the fault feeder selection is a prerequisite for the fault resistance calculation. So it is of some complexity. A simplified algorithm is proposed below.

According to Kirchhoff's current law (KCL), the sum of the residual current variation of all feeders is equal to the variation current of the neutral-to-ground current. The residual current variation of the sound feeder 1 caused by the single-phase-to-ground fault can be calculated as:

$$\dot{I}_{\Delta\mathrm{resS}1} = \dot{U}_{\Delta 0\mathrm{F}} \dot{Y}_{\Sigma 1} \tag{33}$$

Then the residual current variation of the fault feeder *i* caused by the single-phase-to-ground fault can be calculated as:

$$\begin{aligned} \dot{I}_{\Delta\mathrm{resF}i} &= \dot{U}_{0\mathrm{F}}(\dot{Y}_{\Sigma i} + G_\mathrm{F}) - \dot{U}_0 \dot{Y}_{\Sigma i} \\ &= -\dot{U}_{\Delta 0\mathrm{F}}(\dot{Y}_{\mathrm{Y}\Sigma} - \dot{Y}_{\Sigma i}) \end{aligned} \tag{34}$$

From (32) and (34), the faulted current can be recalculated as:

$$\dot{I}_\mathrm{F} = -\dot{U}_{\Delta 0\mathrm{F}} \dot{Y}_{\mathrm{Y}\Sigma} \tag{35}$$

If the single-phase ground fault occurred on phase A, the fault resistance can be calculated as:

$$R_\mathrm{F} = \frac{\dot{U}_{0\mathrm{F}} + \dot{E}_\mathrm{A}}{-\dot{U}_{\Delta 0\mathrm{F}} \dot{Y}_{\mathrm{Y}\Sigma}} \tag{36}$$

In (36), it is not necessary to measure the residual current variation of the fault feeder. So it is not necessary to select the fault feeder. Since the fault current $\dot{I}_\mathrm{F}$ has the same phase-angle with the fault phase-voltage $\dot{U}_{0\mathrm{FA}} = \dot{U}_{0\mathrm{F}} + \dot{E}_\mathrm{A}$, the fault phase can be selected by comparing the phase-angle.

In distribution systems, the normal switching events (such as switching on/off a feeder) are essential. In order to measure the fault resistance adaptively, the total zero-sequence admittance of the network (i.e., $\dot{Y}_{\mathrm{Y}\Sigma}$) should be recalculated after the switching events. At present, many algorithms for the total zero-sequence admittance measurements in a non-direct grounded system have been proposed [19], [26].

B. Protection Algorithm of Fault Feeder Selection

In order to select the fault feeder, [27] has proposed a ground fault protection method based on the zero-sequence calculated admittance. In [27], the asymmetry of the network was not taken into account. The zero-sequence calculated admittance of the sound feeder $\dot{Y}_{0\mathrm{S}1}$ and the fault feeder $\dot{Y}_{0\mathrm{F}i}$ were calculated respectively, as:

$$\dot{Y}_{0\mathrm{S}1} = \frac{\dot{I}_{\mathrm{resS}1}}{\dot{U}_{0\mathrm{F}}} = \dot{Y}_{\Sigma 1} \tag{37}$$

$$\dot{Y}_{0\mathrm{F}i} = \frac{\dot{I}_{\mathrm{resF}i}}{\dot{U}_{0\mathrm{F}}} = \dot{Y}_{\Sigma i} - \dot{Y}_{\mathrm{Y}\Sigma} \tag{38}$$

From (37) and (38), the zero-sequence calculated admittance is equivalent to the residual admittance. However, almost all networks are asymmetrical, so this method suffers from the disadvantage of low accuracy in the condition of the high-resistance-earth fault. And comparing (27) with (37), and (28) with (38), this method can only be used in the case of a metallic single-phase earth fault. An improved measurement of zero-sequence calculated admittance is proposed below which can eliminate the deviation introduced by the asymmetry of the network.

1) Zero-sequence Calculated Admittance of the Sound Feeder

From (12) and (19), the improved zero-sequence calculated admittance of the sound feeder 1 can be calculated as:

$$\dot{Y}_{\Sigma 1} = \frac{\dot{I}_{\Delta\mathrm{resS}1}}{\dot{U}_{\Delta 0\mathrm{F}}} \tag{39}$$

where $\dot{I}_{\Delta\mathrm{resS}1} = \dot{I}_{\mathrm{resS}1} - \dot{I}_{\mathrm{res}1}$, $\dot{I}_{\Delta\mathrm{resS}1}$ is the residual current variation of the sound feeder 1 caused by the earth fault.

2) Zero-sequence Calculated Admittance of the Fault Feeder

From (12) and (18), the residual current variation of the fault feeder *i* can be calculated as:

$$\dot{I}_{\Delta\mathrm{resF}i} = \dot{I}_{\mathrm{resF}i} - \dot{I}_{\mathrm{res}i} = \dot{U}_{\Delta 0\mathrm{F}} \dot{Y}_{\Sigma i} + \dot{I}_\mathrm{F} \tag{40}$$

From (35) and (40), the improved zero-sequence calculated admittance of the fault feeder *i* can be calculated as:

$$\dot{Y}_{\Sigma i} - \dot{Y}_{\mathrm{Y}\Sigma} = \frac{\dot{I}_{\Delta\mathrm{resF}i}}{\dot{U}_{\Delta 0\mathrm{F}}} \tag{41}$$

Based on the above analysis, the fault feeder can be selected by comparing the zero-sequence calculated admittance. In particular, the zero-sequence calculated admittance of the sound feeder is equal to its zero-sequence admittance, but the zero-sequence calculated admittance of the fault feeder is equal to the value that its zero-sequence admittance minus the total zero-sequence admittance of the network. In addition, as the improved fault feeder selection algorithm only needs to measure the variation of each feeder's residual current, the switching events have nothing to do with

the algorithm as well as the fault resistance and the asymmetry of the network.

V. Simulation Analysis

In order to validate the low-current fault detection algorithms proposed, extensive simulation tests have been run by using the Matlab/Simulink shown in Fig. 3. The simulation system is a 10 kV distribution network whose angular frequency is 50Hz. The simulation system has three feeders. Different neutral grounded modes were considered. The influences of the unbalanced distribution parameters were also investigated. Performance of the protection against earth faults was assessed. The zero sequence parameters of the simulation system are listed in Table I.

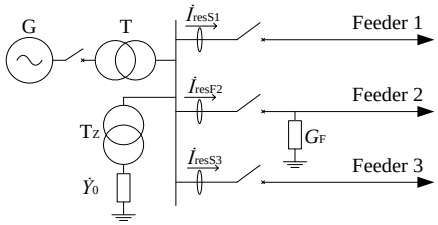

Fig. 3. The radial operated distribution simulation system with a faulty feeder

TABLE I
Zero Sequence Parameters of the Simulation System

Name		Feeder1	Feeder 2	Feeder 3	Whole Network
Capacitance	C_A(μF)	4.064	6.107	3.343	13.514
	C_B(μF)	4.071	5.819	3.027	12.917
	C_C(μF)	4.243	6.285	3.161	13.689
Resistance	R_A(kΩ)	43.085	28.694	56.37	13.193
	R_B(kΩ)	42.974	28.694	56.306	13.179
	R_C(kΩ)	42.717	28.530	56.054	13.106
Capacitive current i_C(A)		22.451	33.031	17.287	72.770
Resistance current i_R(A)		0.404	0.605	0.308	1.316
damping/%		1.797	1.831	1.781	1.809
mismatch/%		1.420	2.238	2.885	1.750

TABLE II
Theoretical and Simulation Results of the Natural Unbalanced Voltage and the Natural Unbalance Currents

Name		Feeder1	Feeder 2	Feeder 3	Whole Network
Theoretical value of U_{bd}	Amplitude (V)	81.963 290	129.229 401	166.554 650	101.049 452
	Phase angle (°)	−57.170 171	−96.782 516	−153.974 722	−106.546 771
Simulation value of U_{bd}	Amplitude (V)	81.963 289	129.229 401	166.554 649	101.049 450
	Phase angle (°)	−57.170 179	−96.782 526	−153.974 733	−106.546 780
Theoretical value of I_{bd}	Amplitude (A)	0.318779	0.7394 653	0.498 786	1.273 842
	Phase angle (°)	31.800 177	−7.831 441	−64.995 289	−17.583 013
Simulation value of I_{bd}	Amplitude (A)	0.318 784	0.739 478	0.498 794	1.273 864
	Phase angle (°)	31.800 173	−7.831 446	−64.995 295	−17.583 019

According to the simulation system parameters listed in Table I, theoretical values of the natural unbalanced voltage $\dot{U}_{bd}$ and the natural unbalance currents $\dot{I}_{bd}$ were calculated respectively by using (1) and (4). Simulation values of the natural unbalanced voltage $\dot{U}_{bd}$ and the natural unbalance current $\dot{I}_{bd}$ were measured respectively in the simulation system. Theoretical and simulation results are shown in Table II.

1) Component Analysis of the Residual Current

According to the parameters of the simulation system in Table I, the quotient $\dot{\tau}_i$ in (14) can be calculated. And according to the natural unbalance currents in Table II, the theoretical results of the residual currents can be calculated by using (14). Theoretical and simulation results of the residual currents of each feeder in the resistance grounded system are shown in Table III. The ground resistance is 800Ω.

TABLE III
Component Analysis of the Residual Current in the Resistance Grounded System

Name		Feeder1	Feeder 2	Feeder 3
Quotient τ_i	Amplitude	0.306474	0.450 900	0.235 983
	Phase angle (deg)	5.658 430	5.639 157	5.667 515
Theoretical value of I_{res}	Amplitude (A)	0.272 320	0.171 586	0.398 767
	Phase angle (deg)	-65.934 245	6.058 497	77.943 170
Simulation value of I_{res}	Amplitude (A)	0.272 325	0.171 589	0.398 773
	Phase angle (deg)	-65.934 327	6.058 732	77.943 140
Amplitude relative error(%)		-0.001 705	-0.001 620	-0.001 432
Phase angle relative error(%)		-0.000 123	-0.003 880	0.000 040

Table VI shows that (14) can calculate the residual current accurately which illustrates that the component analysis of the residual current is correct.

2) Component Analysis of Residual Admittance

As the natural unbalance currents are presented in Table II, $\dot{I}_{bdi}/\dot{I}_{bd\Sigma}$ can be calculated. And according to the simulation system parameters in Table I, the theoretical results of the feeder residual admittances can be calculated by using (24). Theoretical and simulation results of the residual admittances of each feeder in the resistance grounded system are shown in Table IV. The neutral ground resistance is also 800Ω.

TABLE IV
Component Analysis of Residual Admittance in Resistance Grounded System

Name		Feeder1	Feeder 2	Feeder 3
$I_{bdi}/I_{bd\Sigma}$	Amplitude	0.250250	0.580 500	0.391 560
	Phase angle (deg)	49.383 190	9.751 572	−47.412 276
Theoretical value of Y_{res}	Amplitude ($\times 10^{-3}$S)	2.712 939	1.709 395	3.972 643
	Phase angle (deg)	34.960 686	−73.046 571	178.838 100
Simulation value of Y_{res}	Amplitude ($\times 10^{-3}$S)	2.712 981	1.709 420	3.972 694
	Phase angle (deg)	34.960 692	−73.046 249	178.838 155
Amplitude relative error (%)		−0.001 562	−0.001 477	−0.001 290
Phase angle relative error (%)		−0.000017	0.000 442	−0.000 031

Table IV shows that (24) can calculate the residual admittance accurately which illustrates that the component analysis of the residual admittance is correct.

In addition, according to the simulation system parameters in Table I, the zero-sequence admittances of feeder 1, feeder 2, and feeder 3 are $3.889\,2914\times10^{-3}$S, $5.722\,113\times10^{-3}$S, and $2.994\,727\times10^{-3}$S respectively, which have big differences with the residual admittances in Table VII. The reason is the influence of the asymmetry of the network. And this is also the reason why reference [27] cannot select the fault feeder accurately in the high-impedance ground fault.

3) Fault Resistance Measurement

The single-phase-to- ground fault was set in feeder 2 (phase A). The fault resistance is 1 500Ω. The zero-sequence voltage variations $\dot{U}_{\Delta 0F}$ caused by the single-phase earth fault in different neutral point grounded conditions were measured. And the theoretical results of the fault current can be calculated by using (35). Theoretical and simulation results of the fault currents are listed in Table V.

TABLE V
FAULT-CURRENT MEASUREMENT IN DIFFERENT NEUTRAL POINT GROUNDED CONDITIONS

Name		Neutral Point Grounded Conditions			
		Ungrounded	Resistance (R=800Ω)	Petersen Coil (v [a]=−15%)	Petersen Coil in Parallel with Resistance (v=0%, R=400Ω)
$U_{\Delta 0F}$	Amplitude (V)	303.133 519	300.103 013	1938.399 717	1221.587 413
	Phase Angle (deg)	−86.905 962	−81.324 723	70.420 747	−1.302 286
Theoretical value of I_F	Amplitude (A)	3.821 341	3.808 436	3.691 307	3.332 466
	Phase angle (deg)	2.057 797	1.987 197	−12.703 419	−1.302 286
Simulation value of I_F	Amplitude (A)	3.821 378	3.797 087	3.690 930	3.332 437
	Phase Angle (deg)	2.057 785	1.883 774	−12.702 814	−1.298 787
Amplitude relative error(%)		−0.000 956	0.297 988	0.010 104	0.000 880
Phase angle relative error(%)		0.000 594	5.204 423	0.004 761	0.268 711

[a] v is the resonance deviation of the compensation network.

Table V shows that (35) can calculate the fault current accurately which is much more simplified than the ADD algorithm. Then the phase angles of phase A, B, and C were measured. As the phase angle of phase A is equal to the phase angle of the fault current, the fault phase can be selected. And the fault resistance can be calculated by using (36). Simulation results of the fault phase selection and fault resistance measurement are listed in Table VI.

TABLE VI
THE FAULT PHASE SELECTION AND FAULT RESISTANCE MEASUREMENT IN DIFFERENT NEUTRAL POINT GROUNDED CONDITIONS

Name		Neutral Point Grounded Conditions			
		Ungrounded	Resistance (R=800Ω)	Petersen coil (v=−15%)	Petersen Coil in Parallel with Resistance (v=0%, R=400Ω)
Phase angle (°)	Phase A	2.057 785	1.987 222	−12.702 839	−1.298 791
	Phase B	−121.448 025	−121.572 673	−117.664 954	−125.615 740
	Phase C	119.387 937	119.583 785	130.750 731	126.853 788
Fault current		2.057 797	1.987 197	−12.703 419	−1.302 286
The fault phase?		Phase A	Phase A	Phase A	Phase A
Voltage amplitude of phase A (V)		5732.066 272	5712.707 605	5536.405 263	4998.660 938
The fault resistance		1500.000 006	1504.497 264	1500.001 167	1500.001 767

Table VII shows that the fault current and fault resistance can be calculated only by measuring the variation of the zero-sequence voltage, which is more convenient than DDA.

4) Fault Feeder Selection

The single-phase ground fault was also set in feeder 2 (phase A). According to the simulation system parameters listed in Table I, the zero-sequence calculated admittance of feeder 1, feeder 2, and feeder 3 are $3.889\,2914\times10^{-3}$S, $6.884\,018\times10^{-3}$S, and $2.994\,727\times10^{-3}$S, respectively. The traditional fault feeder selection method based on the zero-sequence calculated admittance which can be calculated by using (37) and (38) was simulated first. Simulation results with different fault resistance (i.e. 10 Ω and 1 500 Ω) are listed in Table VII and Table VIII, respectively.

TABLE VII
TRADITIONAL FAULT FEEDER SELECTION IN DIFFERENT NEUTRAL POINT GROUNDED CONDITIONS WITH 10 Ω FAULT RESISTANCE

Name		Neutral Point Grounded Conditions			
		Ungrounded	Resistance (R=800Ω)	Petersen Coil (v=−15%)	Petersen Coil in Parallel with Resistance (v=0%, R=400Ω)
Feeder1	Amplitude ($\times10^{-3}$S)	3.92546	6.847368	2.921928	3.92546
	Relative error(%)	0.929 961	−0.5323 963	−2.430 890	0.929 961
Feeder2	Amplitude ($\times10^{-3}$S)	3.925845	6.998331	2.920965	3.925845
	relative error(%)	0.939 844	1.660 560	−2.463 067	0.939 844
Feeder3	Amplitude ($\times10^{-3}$S)	3.918 618	7.199 137	2.916 139	3.918 618
	relative error(%)	0.754 028	4.577 537	-2.624 210	0.754 028

TABLE VIII
TRADITIONAL FAULT FEEDER SELECTION IN DIFFERENT NEUTRAL POINT GROUNDED CONDITIONS WITH 1 500 Ω FAULT RESISTANCE

Name		Neutral Point Grounded Conditions			
		Ungrounded	Resistance (R=800Ω)	Petersen Coil (v=−15%)	Petersen coil in Parallel with Resistance (v=0%, R=400Ω)
Feeder1	Amplitude ($\times10^{-3}$S)	5.332 988	9.035 886	4.233 062	5.332 988
	Relative error(%)	37.119 773	31.258 902	41.350 520	37.119 773
Feeder2	Amplitude ($\times10^{-3}$S)	5.383 176	9.300 375	4.088 535	5.38 3176
	relative error(%)	38.410 195	35.100 975	36.524 451	38.410 195
Feeder3	Amplitude ($\times10^{-3}$S)	3.697 387	8.426 913	2.730 330	3.697 387
	relative error(%)	−4.934 171	22.412 705	−8.828 755	−4.934 171

TABLE IX
IMPROVED FAULT FEEDER SELECTION IN DIFFERENT NEUTRAL POINT GROUNDED CONDITIONS WITH 1 500 Ω FAULT RESISTANCE

Name	Neutral Point Grounded Conditions			
	ungrounded	Resistance (R=800Ω)	Petersen Coil (v=−15%)	Petersen Coil in Parallel with Resistance (v=0%, R=400Ω)

Feeder1	Amplitude ($\times10^{-3}$S)	3.889 329	3.980 542	3.889 532	3.889 306
	Relative error(%)	–0.017 110	–2.362 721	–0.022 341	–0.016 519
Feeder2	Amplitude ($\times10^{-3}$S)	6.884 084	6.918 631	7.212 921	6.793 648
	relative error(%)	−0.000 955	−0.502 798	−4.777 775	1.312 759
Feeder3	Amplitude ($\times10^{-3}$S)	2.994 755	2.994 755	2.994 912	2.994 738
	relative error(%)	−0.000 941	−0.000 941	−0.006 191	−0.000 369

From Table VII and Table VIII, in the condition of the high-resistance-earth fault (i.e. 1 500 Ω), the traditional fault feeder selection method is invalid. However, an improved fault feeder selection method was proposed, and the zero-sequence calculated admittance can be calculated by using (39) and (41). Simulation results with a 1 500 Ω fault resistance are listed in Table IX. Table IX shows that (39) and (41) can calculate the zero-sequence calculated admittance accurately, and the improved fault feeder selection method will not be affected by the fault resistance, neutral point grounded conditions, and the asymmetry of the network.

VI. Conclusion

In this paper, several algorithms for single-phase-to-ground fault detection with distributed parameters analysis in a non-direct grounded system were proposed. The novel generating mechanisms of zero-sequence voltage and residual current enrich the phase-sequence-analysis theory. The residual current and the residual admittance in the fault network can be decomposed into three separate parts. According to the component analysis of the residual admittance, the phase relationship between the residual current and zero-sequence voltage can also be recognized more accurately. The fault current and fault resistance can be calculated accurately only by measuring the zero-sequence voltage variation caused by the single-phase earth fault. It no longer needs the prerequisites of the faulty feeder selection and the fault feeder's zero-sequence admittances measurement. And the fault phase can also be selected. The fault feeder can be selected by comparing the zero-sequence calculated admittance, which only needs to measure each feeder's residual current variation. The improved fault feeder selection method will not be affected by the fault resistance and the asymmetry of the network.

References

[1] K.J. Sagastabeitia, I. Zamora, A.J. Mazón, Z. Aginako, and G. Buigues, "Low-current fault detection in high impedance grounded distribution networks, using residual variations of asymmetries," IET Gene. Trans. & Distr., vol. 6, no.12, pp. 1252–1261, Dec. 2012.

[2] D. Griffel, V. Leitloff, Y. Harmand, and J. Bergeal, "A new deal for safety and quality on MV networks," IEEE Trans. Power Deli., vol.12, no.4, pp. 1428–1433, Oct.1997.

[3] Z. Xiangjun, Y. Kun, W. Yuanyuan, and X. Yao, "A novel single phase grounding fault protection scheme without threshold setting for neutral ineffectively earthed power systems," CSEE Journal of Power and Energy Systems, vol. 2, no.3, pp. 73–81, Sep. 2016.

[4] M. Givelberg, E. Lysenko, and R. Zelichonok, "Zero sequence directional earth-fault protection with improved characteristics for compensated distribution networks," Elect. Power Sys. Res., vol. 52, no.3, pp.217–222, Dec. 1999.

[5] Z. Xiangjun, K.K. Li, W.L. Chan, Su. Sheng, and W. Yuanyuan, "Ground-Fault Feeder Detection With Fault-Current and Fault-Resistance Measurement in Mine Power Systems," IEEE Trans. Indus. Elec., vol. 44, no. 2, pp. 424–429, Mar./Apr. 2008.

[6] T. Welfonder, V. Leitloff, R. Fenillet, and S. Vitet, "Location strategies and evaluation of detection algorithms for earth faults in compensated MV distribution systems," IEEE Trans on Power Del., vol.15, no.4, pp.1121-1128, 2000.

[7] V. Leitloff, R. Feuille, and D. Griffel, "Detection of resistive single-phase earth faults in a compensated power-distribution system," Eur. Trans. Elect. Power, vol. 7, no.1, pp. 65–73, Jul./Feb. 1997.

[8] I. Zamora, A.J. Mazon, K.J. Sagastabeitia, and J.J. Zamora, "New method for detecting low current faults in electrical distribution systems," IEEE Trans. Power Del., vol. 22, no. 4, pp. 2072–2079, Oct. 2007.

[9] F. Ruz, A. Quijano, and E. Gomez, "DSTRP: A New Algorithm for High Impedance Fault Detection in Compensated Neutral Grounded M.V. Power Systems," Eur. Trans. Elect. Power, vol. 13, no.1, pp. 23–28, Jan./Feb. 2003.

[10] K.J. Sagastabeitia, I. Zamora, A.J. Mazón, Z. Aginako, and G. Buigues, "Phase asymmetry: a new parameter for detecting single-phase earth faults in compensated MV networks," IEEE Trans. Power Deli., vol. 26, no. 4, pp. 2251–2258, Oct.2011.

[11] S. Hanninen, M. Lehtonen, and U. Pulkkinen, "A probabilistic method for detection and location of very high resistive earth faults," Elect. Power Sys. Res., vol. 54, no.3, pp.199–206, Jun. 2000.

[12] Y. Sheng and S.M. Rovnyak, "Decision tree-based methodology for high impedance fault detection," IEEE Trans. Power Del., vol. 19, no. 2, pp. 533–536, Apr. 2004.

[13] A.H. Etemadi, and M. Sanayepasand, "High-impedance fault detection using multi-resolution signal decomposition and adaptive neural fuzzy inference system," IET Gene., Trans. & Distr., vol. 2, no. 1, pp. 110–118, Jan. 2008.

[14] C.J. Kim, L. Seungjae, and K. Sanghee, "Evaluation of feeder monitoring parameters for incipient fault detection using Laplace trend statistic," IEEE Trans. Ind. Appl., vol. 40, no. 6, pp. 1718–1724, Nov./Dec. 2004.

[15] D. Xinzhou, W. Jun, S. Shenxing, W. Bin, B. Dominik, and M. Redefern, "Traveling wave based single-phase-to-ground protection method for power distribution system," CSEE Journal of Power and Energy Systems, vol. 1, no.2, pp. 75–82, Jun. 2015.

[16] M.F. Abdel-Fattah, and M. Lehtonen, "Transient algorithm based on earth capacitance estimation for earth-fault detection in medium-voltage networks," IET Gene. Trans. & Distr., vol. 6, no.2, pp. 161–166, Feb. 2012.

[17] M. Michalik, W. Rebizant, M. Lukowicz, L. Seungjae, and K. Sanghee, "High-impedance fault detection in distribution networks with use of wavelet-based algorithm," IEEE Trans. Power Del., vol. 21, no. 4, pp. 1793–1802, Oct. 2006.

[18] L. Jiping, L. Jian, and L. Wenyuan, "A new approach to identifying faulty lines in distribution systems based on traveling wave refraction and coupling," Elect. Power Sys. Res., vol. 78, no.3, pp.353–360, Mar. 2008.

[19] Z. Xiangjun, X. Yao, and W. Yuanyuan, "Some novel techniques for insulation parameters measurement and Petersen-coil control in distribution systems," IEEE Trans. Indus. Elec., vol. 57, no. 4, pp. 1445–1451, Apr.2010.

[20] Y. Huannian, The Resonance Grounding of the Electronic System. Beijing, China: China Electron. Power Press, 2001, pp. 34–36.

[21] Z. Qingchao, Z. Yao, S. Wennan, and F. Dazhong, "Transmission line fault location for single-phase-to-earth fault on non-direct-ground neutral system," IEEE Trans. Power Del., vol.13, no. 4, pp. 1086–1092, Oct. 1998.

[22] Z. Xiangjun, K.K. Li, W.L. Chan, and Y. Xianggen, "On-site safety evaluation for earth fault in mining power systems," IEEE Trans. Ind. Appl., vol. 39, no. 6, pp. 1563–1569, Nov./Dec. 2003.

[23] K.Y. Lien, S.L. Chen, C.J. Liao, T.Y. Guo, T.M. Lin, and J.S. Shen, "Energy variance criterion and threshold tuning scheme for high impedance fault detection," IEEE Trans. Power Del., vol.14, pp. 810–817, Jul. 1999.

[24] I. Zamora, A.J. Mazón, K.J. Sagastabeitia, O. Picó, and J.R. Saenz, "Verifying resonant grounding in distribution systems, " *IEEE Comput. Appl. Power*, vol.15, no. 4, pp.45–50, Oct. 2002.

[25] V. Leitloff, "Etude, Conception et Réalization d'un Automate de Gestion de Réseaux MT Compensés," Ph.D. dissertation, Inst. Nat. Polytech. de Grenoble (INPG), France, 1994.

[26] L. Baowen, M. Hongzhong, S. Peifeng, and C. Bingbing, "New flexible control system of full compensation single-phase ground fault fundamental current," Proc. CSEE, vol. 36, no. 9, pp. 2322–2330, 2016, (in Chinese).

[27] Z. Xiangjun, Y. Xianggen, Z. Zhe, C. Deshu, and W. Minghao, “Study on feeder grounding fault protection based on zero sequence admittance,” Proc. CSEE, vol. 21, no. 4, pp. 5–10, Apr. 2001(in Chinese).

Baowen Liu received his B.S. degree from University of Jinan in 2011and M.S. degree from China University of Mining & Technology, in 2014, respectively. he is currently working toward the Ph.D. degree in the Hohai University. His research interests include distribution system control and protection, and fault diagnosis of electrical equipment.

Hongzhong Ma received a B.S. (1989), M.S. (1994) and Ph.D (2002) from Southeast University of China.

Currently, he is a professor at Hohai University. He is also the Director of the Department of Electrical Engineering, Hohai University, China. His primary research interests are condition monitoring and fault diagnosis of electrical equipment, Electrical machines and drives, and power system research.

Honghua Xu received a B.S.(2004), M.S.(2007) and Ph.D.(2011) from the Institute of Microelectronics, Peking University, Beijing, China.

Since 2011, he has been with the Nanjing Power Supply Company, Jiangsu Electric Power Company, Aoti Street 1#, Nanjing, Jiangsu, China. His research interests focus on condition monitoring and fault diagnosis of power systems, smart grids and the integration of renewable energy sources in the grid.

Ping Ju was born in China in 1962. He received B.Sc. and M.Sc. degrees from Southeast University, Nanjing, China in 1982 and 1985, respectively, and a Ph.D. degree from Zhejiang University, Hangzhou, China, all in electrical engineering. From 1994 to 1995, he was an Alexander-von-Humboldt Fellow at the University of Dortmund, Germany. He is currently a Professor of electrical engineering with Hohai University, Nanjing, China. His research interests include high voltage insulation technology, modeling and control of power systems.